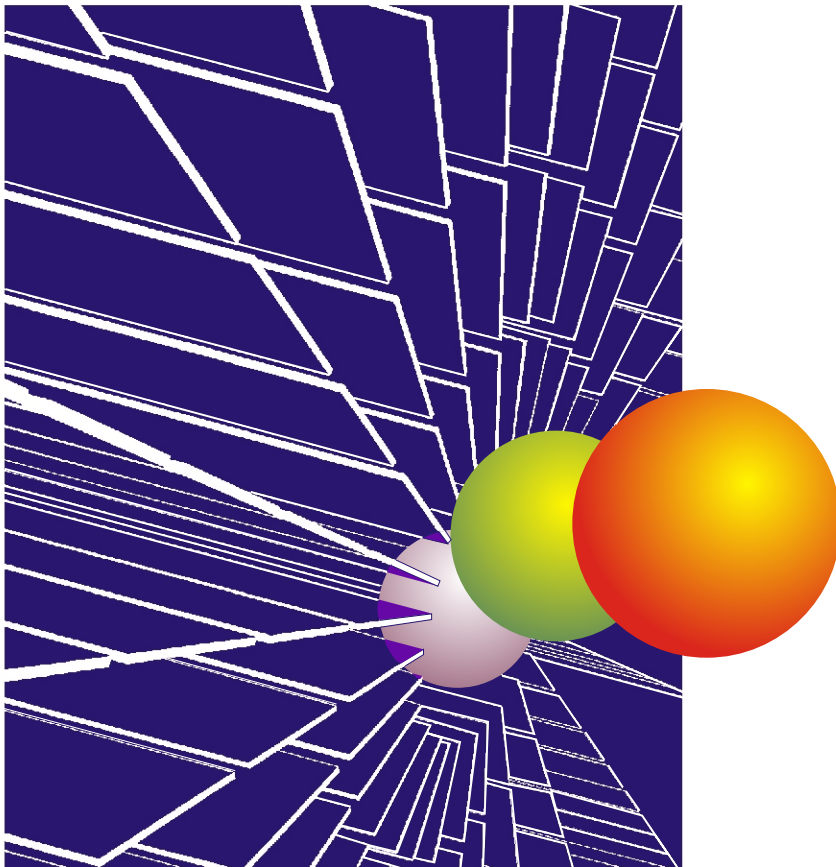


# **Construction and Long-Term Monitoring of a Concrete Box Culvert Bridge Reinforced with GFRP Bars**

RI 99-028



December, 2001

## TECHNICAL REPORT DOCUMENTATION PAGE

<b>1. Report No.</b> RDT01-016	<b>2. Government Accession No.</b>	<b>3. Recipient's Catalog No.</b>
<b>4. Title and Subtitle</b> Construction and Long-Term Monitoring of a Concrete Box Culvert Bridge Reinforced with GFRP Bars		<b>5. Report Date</b> November 2001
<b>7. Author/s</b> T. Alkhrdaji and A. Nanni		<b>6. Performing Organization Code</b> UMR
<b>9. Performing Organization Name and Address</b> Center for Infrastructure Engineering Studies University of Missouri - Rolla 223 ERL Rolla, MO 65409		<b>8. Performing Organization Report No.</b> RDT01-016/RI99-028
<b>12. Sponsoring Organization Name and Address</b> MODOT Research Development and Technology 1617 Missouri Blvd., Jefferson City, MO 65109 University TC 223 Engineering Research Lab., Rolla, MO 65409		<b>10. Work Unit No. (TRAIS)</b>
		<b>11. Contract or Grant No.</b>
		<b>13. Type of report and period covered</b> Technical Report; 09/99-05/01
		<b>14. Sponsoring Agency Code</b> MoDOT
<b>15. Supplementary Notes</b> This investigation was conducted in cooperation with the U.S. Department of Transportation.		
<b>16. Abstract</b> <p>This report presents the design, construction, and laboratory/field testing of a box culvert bridge reinforced with glass FRP (GFRP) bars. The concrete box culvert units were designed for maximum loads determined in accordance with AASHTO design guidelines. A concrete precaster fabricated the box culvert units that were reinforced entirely with GFRP bars pre-bent and cut to size by the manufacturer. Two specimens were tested to failure in the laboratory to verify their design and performance. Deformations and reinforcement strains were measured throughout the tests. Test results compared well with theoretical values. The bridge was installed and opened to traffic in October 1999. The long-term performance of the bridge is being monitored through periodic in-situ load tests. The first load test was conducted eight months after bridge construction while the second test was conducted 20 months thereafter. In each test, a truck was used to load the bridge and the elastic response of the bridge was measured. The two load tests indicated that bridge deflections were small. After applied load was removed, the bridge rebound indicated elastic behavior. Comparison of the results of the two tests indicates that no significant degradation of stiffness occurred during 12 months.</p>		
<b>17. Key Words</b> Box culvert, bridge, concrete, glass FRP, internal reinforcement, load testing,	<b>18. Distribution Statement</b> No restrictions. This document is available to the public through NTIC, Springfield, VA 22161	
<b>19. Security Classification (of this report)</b> Unclassified	<b>20. Security Classification (of this page)</b> Unclassified	<b>21. No. of Pages</b> 44



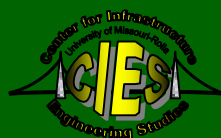
# CENTER FOR INFRASTRUCTURE ENGINEERING STUDIES

## CONSTRUCTION AND LONG-TERM MONITORING OF A CONCRETE BOX CULVERT BRIDGE REINFORCED WITH GFRP BARS

by

**Tarek Alkhrdaji**  
**Antonio Nanni**

**August 2001**



**CIES**  
**XX-XX**

### **DISCLAIMER**

The contents of this report reflect the views of the author(s), who are responsible for the facts and the accuracy of information presented herein. This document is disseminated under the sponsorship of the Center for Infrastructure Engineering Studies (CIES), University of Missouri-Rolla, in the interest of information exchange. CIES assumes no liability for the contents or use thereof.

The mission of CIES is to provide leadership in research and education for solving society's problems affecting the nation's infrastructure systems. CIES is the primary conduit for communication among those on the UMR campus interested in infrastructure studies and provides coordination for collaborative efforts. CIES activities include interdisciplinary research and development with projects tailored to address needs of federal agencies, state agencies, and private industry as well as technology transfer and continuing/distance education to the engineering community and industry.

Center for Infrastructure Engineering Studies (CIES)  
University of Missouri-Rolla  
223 Engineering Research Laboratory  
1870 Miner Circle  
Rolla, MO 65409-0710  
Tel: (573) 341-6223; fax -6215  
E-mail: [cies@umr.edu](mailto:cies@umr.edu)  
[www.umar.edu/~cies](http://www.umar.edu/~cies)

RESEARCH INVESTIGATION RI99-028

CONSTRUCTION AND LONG-TERM MONITORING OF  
A CONCRETE BOX CULVERT BRIDGE  
REINFORCED WITH GFRP BARS

PREPARED FOR THE  
MISSOURI DEPARTMENT OF TRANSPORTATION

IN COOPERATION WITH THE  
U.S. DEPARTMENT OF TRANSPORTATION  
FEDERAL HIGHWAY ADMINISTRATION

Written By:

Tarek Alkhrdaji, Ph.D. Candidate  
Antonio Nanni, V. & M. Jones Professor  
CENTER FOR INFRASTRUCTURE ENGINEERING STUDIES  
UNIVERSITY OF MISSOURI – ROLLA

Submitted  
August 2001

The opinions, findings and conclusions expressed in this report are those of the principal investigator and the Missouri Department of Transportation. They are not necessarily those of the U.S. Department of Transportation, Federal Highway Administration. This report does not constitute a standard, specification or regulation.

# **CONSTRUCTION AND LONG-TERM MONITORING OF A CONCRETE BOX CULVERT BRIDGE REINFORCED WITH GFRP BARS**

## **EXECUTIVE SUMMARY**

This report presents the design, construction, and laboratory/field testing of a box culvert bridge reinforced with glass FRP (GFRP) bars. The bridge was constructed to replace a bridge built in the early 1970's that consisted of three concrete-encased corrugated steel pipes. Due to excessive corrosion of the steel pipes, the original bridge became unsafe to operate. The new concrete box culvert units were designed for maximum loads determined in accordance with AASHTO design guidelines.

A concrete precaster fabricated the box culvert units that were reinforced entirely with GFRP bars pre-bent and cut to size by the manufacturer. Two specimens were tested in the lab to verify their design and performance. The boxes were subjected to quasi-static loading cycles up to failure. Deformations and reinforcement strains were measured throughout the tests.

Test results compared well with theoretical values. The new bridge was installed and opened to traffic in October 1999. The long-term performance of the new bridge is being monitored through periodic in-situ load tests. The first load test was conducted eight months after bridge construction while the second test was conducted 20 months thereafter. In each test, a truck was used to load the bridge and the elastic response of the bridge was measured. The two load tests indicated that bridge deflections were small. After applied load was removed, the bridge rebound indicated elastic behavior. Comparison of the results of the two tests indicates that no significant degradation of stiffness occurred during 12 months.

## **ACKNOWLEDGMENTS**

The project was made possible with the financial support received from the Missouri Department of Transportation, UMR - University Transportation Center on Advanced Materials and NDT Technologies, and the City of Rolla. Hughes Brothers, Inc., Omaha, Nebraska provided the GFRP bars. Scurlock Industries of Springfield, Missouri, fabricated the box units.



## TABLE OF CONTENTS

EXECUTIVE SUMMARY .....	iv
ACKNOWLEDGMENTS .....	v
LIST OF ILLUSTRATIONS .....	vii
LIST OF TABLES .....	viii
1. Introduction.....	1
1.1. General.....	1
1.2. Objectives .....	1
1.3. Background on Fiber Reinforced Polymers.....	1
1.3.1. FRP Composites.....	1
1.3.2. FRP for Internal Reinforcement.....	1
1.3.3. History of Use .....	2
1.4. Walker Bridge.....	2
2. GFRP Box Culvert Design.....	3
2.1. General.....	3
2.2. Design of a Box Culvert Unit .....	3
2.2.1. Analysis for Internal Force .....	3
2.3. GFRP Design Method.....	3
2.3.1. ACI Design Guide.....	4
3. Fabrication and installation of the box culvert units.....	8
4. Laboratory verification .....	11
4.1. General.....	11
4.2. Test Set-up and Instrumentation .....	11
4.3. Test Results and Discussion .....	12
4.4. Numerical Model .....	14
4.5. Comparison with Proposed Design Approach by ACI Committee 440H .....	15
5. Bridge Construction .....	17
6. Field load Testing .....	18
6.1. General.....	18
6.2. Instrumentation .....	18
6.3. Load Testing .....	19
6.4. Test Results.....	20
6.5. Load Deflection Characteristics.....	22
6.6. Summary .....	26
7. CONCLUSIONS.....	27
8. References.....	28
Appendix A: Bridge Location.....	30
Appendix B: Selected Output of BoxCar.....	31

## LIST OF ILLUSTRATIONS

Figure 1.1	Old Walker Bridge.	2
Figure 2.1	Details and GFRP reinforcement for box culvert.	7
Figure 3.1	Rig of wood for GFRP cage assembly.	8
Figure 3.2	Finished GFRP cage.	9
Figure 3.3	Strain gage on a GFRP bar.	9
Figure 3.4	Casting form.	10
Figure 3.5	Plastic wheel spacers.	10
Figure 3.6	A typical tongue and groove rectangular box section.	10
Figure 4.1	Test setup and instrumentation.	11
Figure 4.2	Cracking locations.	12
Figure 4.3	Mid-span deflection of Box 1.	12
Figure 4.4	Mid-span deflection of Box 2.	13
Figure 4.5	Strain measured at mid-span of Box 1.	13
Figure 4.6	Strain measured at end of top panel for Box 1.	14
Figure 4.7	Theoretical moment distribution at maximum load.	16
Figure 4.8	Comparison of experimental and theoretical load-deflection behavior.	16
Figure 5.1	Bridge construction.	17
Figure 6.1	Test Truck Wheel Loads.	18
Figure 6.2	LVDT Layout and Axles Locations.	19
Figure 6.3	Field Load Testing.	20
Figure 6.4	Deflections of the North Box Due to Front Axle Loading.	23
Figure 6.5	Deflections of the North Box Due to Rear Axle Loading	23
Figure 6.6	Deflections of the South Box Due to Front Axle Loading.	24
Figure 6.7	Deflections of the South Box Due to Rear Axle Loading.	24
Figure 6.8	Adjusted Average for Measurements Taken on the North Box.	25
Figure 6.9	Adjusted Average for Measurements Taken on the South Box.	25
Figure A.1	Current Walker Culvert plan	30

## LIST OF TABLES

Table 6.1	Deflections for the North Box –Test 1.	20
Table 6.2	Deflections for the South Box –Test 1.	21
Table 6.3	Deflections for the North Box –Test 2.	21
Table 6.4	Deflections for the South Box –Test 2.	22

## **1. INTRODUCTION**

### **1.1. General**

Culverts are commonly made from a variety of materials including reinforced concrete (RC), corrugated metal pipes, and stone. Precast RC box culverts are very common and usually constructed as single or multicell culverts. Precast RC box culverts offer advantages such as enhanced quality control, use of higher strength concrete, lower cost due to mass production, and short installation time. Culvert bridges are subject to aggressive environments and combinations of moisture, temperature, and chlorides accelerate the corrosion of the metal pipes or the internal steel reinforcement leading eventually to a structural deficiency. Reinforcing bars made of fiber-reinforced polymers (FRP) are corrosion-resistant and therefore may be suitable for internal reinforcement of RC box culverts.

This report describes the design, construction, performance, and long-term monitoring program of a concrete box culvert bridge reinforced entirely with glass FRP (GFRP) bars. It demonstrates the feasibility of and effectiveness of FRP internal reinforcement to reduce corrosion-related problems, thus increasing the service life of RC culvert bridge structures.

### **1.2. Objectives**

The project aimed at investigating the feasibility and effectiveness of FRP internal reinforcement to reduce corrosion-related problems of RC culvert bridges. The project consisted of design and laboratory verification, field construction, and periodic in-situ load testing of a bridge. RC box units were tested in the laboratory to verify the design approach, serviceability conditions, and their ultimate load capacity.

### **1.3. Background on Fiber Reinforced Polymers**

#### **1.3.1. FRP Composites**

FRP material systems, which are composed of fibers embedded in a polymeric matrix, exhibit several properties suitable for their use as structural reinforcement (Nanni 1993, Nanni and Dolan 1993, ACI Committee 440 1996, El-Badry 1996). FRP composites are anisotropic and characterized by excellent tensile strength in the direction of the fibers. They do not exhibit yielding, but instead are elastic up to failure. FRP composites are corrosion resistant, and therefore should perform better than other construction materials in terms of weathering behavior.

#### **1.3.2. FRP for Internal Reinforcement**

Marshall-Vega led the initial development of GFRP reinforcing bars in the United States for the purpose of reinforcing polymer concrete due to its thermal incompatibility with steel bars (ACI Committee 440 1996). The excellent mechanical properties of FRP materials and their non-corrosive nature have made them suitable for structural reinforcement (Iyer and Sen 1991). The use of FRP composites to reinforce and prestress

concrete structural members was implemented in many projects worldwide (El-Badry 1996, JSCE 1997, Benmokrane and Rahman 1998, and Saadatmanesh and Ehsani 1998, Dolan et al. 1999). Just recently (after the completion of this project), ACI Committee 440 published the “Guide for the Design and Construction of Concrete Reinforced with FRP Bars” (ACI Committee 440, 2001). Similar documents are being produced in several European countries.

### **1.3.3. History of Use**

The Japanese have the largest number of projects involving FRP as internal reinforcement with more than 100 projects and demonstrations. In Germany, programs have been implemented since 1986 to increase the research and use of FRP reinforcement in Europe. The European BRITE/EURAM Project, “Fiber Composite Elements and Techniques as Nonmetallic Reinforcement,” conducted extensive testing and analysis of the FRP materials from 1991 to 1996. Canadian civil engineers are continuing to develop provisions for FRP reinforcement in the Canadian Highway Bridge Design Code and have constructed a number of demonstration projects. The Headingley Bridge in Manitoba (Rizkalla 1997), the Kent County Road No. 10 Bridge (Tadros et al. 1998), and the Joffre Bridge (Benmokrane et al. 1996) are examples of bridges with internal FRP reinforcing bars. In the USA, typical uses of FRP reinforcement have been reported in the literature (ACI Committee 440 1996).

### **1.4. Walker Bridge**

Walker Bridge is located on Walker Avenue in the City of Rolla, Phelps County, Missouri (see Appendix A). Due to corrosion problems, the bridge was scheduled for reconstruction during the Fall of 1999. The existing bridge consisted of three 42-in diameter corrugated steel pipes encased in concrete and situated transverse to the roadway. The bridge was constructed in the 1970’s with an original roadway width of 16 ft (See Figure 1.1).



**Figure 1.1:** Old Walker Bridge.

## 2. GFRP BOX CULVERT DESIGN

### 2.1. General

Steel reinforcement for precast RC box sections was commonly determined using the standard design tables presented in ASTM C 789 for box culverts with more than 2 feet of cover and ASTM C 850 for box culverts with less than 2 feet of cover. These two standards have been recently replaced by ASTM C 1433-00: Standard Specification for Precast Reinforced Concrete Box Sections for Culverts, Storm Drains, and Sewers. The design tables are based on ACI's ultimate strength design method (Heger et al. 1976). Special designs for sizes and conditions other than as tabulated are also possible and should conform to the requirements of the respective specifications (ASTM C 1433-00).

### 2.2. Design of a Box Culvert Unit

#### 2.2.1. Analysis for Internal Force

Based on consideration of hydraulic requirements and site characteristics, the dimensions of the box culvert units were selected to be 5 by 5 ft with a wall thickness of 6 in. Analysis was achieved using BOXCAR (FHWA 1989), a software program that performs structural analysis and design of buried single cell RC box culverts in accordance with AASHTO live load requirements and design requirements (AASHTO 1996). Based on user-specified box geometry, material properties and loading data, the program computes the maximum design moments, shears and thrust forces at critical locations using the stiffness matrix method and provides reinforcement design considering the most severe case of 32 load conditions (FHWA 1989). Using this program, the analysis was carried out on the box unit considering HS15 truck loading and 1.9 ft of cover that included the topsoil and asphalt overlay as per the City of Rolla's specifications. The maximum positive and negative moments due to factored loads were determined to be 35.4 and 26.0 in-k/ft, respectively, at the bottom slab panel of the box unit. The maximum negative moment at the panel's end occurred at the bottom of the wall panel and was equal to 21.3 in-k/ft. Maximum shear and thrust forces were 4.1 and 2.4 kips, respectively. Selected output of BOXCAR program is given in Appendix B.

### 2.3. GFRP Design Method

The internal reinforcement considered for this application consisted of a commercially available #2 GFRP bar with guaranteed tensile strength  $f_{fu}^*$  of 110 ksi, a guaranteed modulus  $E_f$  of 5,900 ksi, and guaranteed rupture strain  $\varepsilon_{fu}^*$  of 1.9%. The design strength of the bar  $f_{fu}$  was taken as  $C_E f_{fu}^*$  (the environmental reduction factor  $C_E$  is a knock-down factor intended to account for changes in tensile strength due to environmental degradation). For the case of GFRP bars in concrete exposed to earth and weather, ACI-440 recommends to take a  $C_E$  equal to 0.7. No reduction factor was applied to the elastic modulus.

Two cases were considered for design: at panel mid-span with ultimate moment demand of 35.4 in-k/ft and at panel ends with ultimate moment demand of 21.3 in-k/ft. For

negative moments (at panel ends), the strength of the FRP bars at the bend was determined using the formula proposed by the Japan Society of Civil Engineers as follows (JSCE 1997):

$$f_{fb} = \left( 0.05 \cdot \frac{r_b}{d_b} + 0.3 \right) f_{fu} \leq f_{fu} \quad (1)$$

For the current design, the specified bend radius  $r_b$  was equal to four bar diameter  $4d_b = 4(0.25\text{in}) = 1\text{ in}$ ; therefore the design strength at the bend was  $f_{fb} = 0.5 f_{fu}$ .

Although the slab section of the box was to be reinforced in a symmetric manner (top and bottom reinforcement), the contribution of compression GFRP reinforcement was disregarded. The design was achieved based on principles of equilibrium and compatibility, and the constitutive laws of the materials. A strength reduction factor  $\phi$  of 0.75 was used for both flexure and shear. Using this approach, a design concrete strength of 5,000 psi, and GFRP area of 0.15 in<sup>2</sup>/ft (#2 @ 4 in. c/c), the design strength  $\phi M_n$  of panel was 41.8 in-k/ft and 21.5 in-k/ft at mid-span and supports, respectively. Under service load, the maximum stress computed in the GFRP bars was 22.3 ksi (0.29  $f_{fu}$ ). The corresponding crack width at service level was approximately 0.02 in.

For ease of construction, it was decided to use U-shaped FRP bars, overlapped at the sides of the box. The development length of the FRP bars was determined using a conservative formula that was based on test results available in the literature as follows (Ehsani et al. 1996 and Gao et al. 1998):

$$\lambda_{df} = \frac{d_b f_{fu}}{2700} \quad (2)$$

where  $f_{fu}$  is in psi. The length of a lap-splice was determined using  $1.6\lambda_{df}$  as proposed by Benmokrane et al. (1997). Using Eq. (2), the required development length was  $\lambda_{df} = 7\text{ in}$ . Accordingly, the required lap-splice length was 11.4 in; however, a lap-splice length of 16 in was used. As per AASHTO recommendations (AASHTO 1996), transverse reinforcement was provided in the top panel (#2 @ 4 in GFRP bars) to ensure load distribution. Transverse reinforcement (#2 @ 8 in GFRP bars) was also provided in the walls and bottom panel to facilitate the GFRP reinforcing cage construction and load distribution. The final design of the box culvert unit is shown in Figure 2.1.

### 2.3.1. ACI Design Guide

The following section summarizes some of the requirements of the ACI guidelines. Some differences may be noted between the guide and the coefficient adopted for this project.

Design values. The design tensile strength that should be used in all design equations is given as  $f_{fu} = C_E f_{fu}^*$ , where:  $f_{fu}$  = design tensile strength of FRP, considering reductions for service environment;  $C_E$  = environmental reduction factor. The factor is a function of fiber type and exposure condition (in the case of glass the values are 0.8 and 0.7 for internal and external exposures, respectively); and  $f_{fu}^*$  = guaranteed tensile strength of an FRP bar defined as the mean tensile strength of a sample of test specimens

minus three times the standard deviation ( $f_{fu}^* = f_{u,ave} - 3\sigma$ ). The design rupture strain should be determined similarly, whereas the design modulus of elasticity is the same as the value reported by the manufacturer. Design parameters in compression are not addressed since the use of FRP rebars in this instance is discouraged.

Behavior and failure modes in flexure. The non-ductile behavior of FRP reinforcement necessitates a reconsideration of this approach. If FRP reinforcement ruptures, failure of the member is sudden and catastrophic. However, there would be some limited warning of impending failure in the form of extensive cracking and large deflection due to the significant elongation that FRP reinforcement experiences before rupture. The concrete crushing failure mode is marginally more desirable for flexural members reinforced with FRP bars (Nanni 1993) since the member does exhibit some plastic behavior before failure. In conclusion, both failure modes (i.e., FRP rupture and concrete crushing) are acceptable in governing the design of flexural members reinforced with FRP bars provided that strength and serviceability criteria are satisfied. To compensate for the lack of ductility, the member should possess a higher reserve of strength. The suggested margin of safety against failure is therefore higher than that used in traditional steel-RC design. Based on the choice of  $\Phi$  factors (see section below) this margin can vary between 1.3 and 1.8.

$\Phi$  factor for flexure. When concrete crushing controls, a conservative strength-reduction factor of 0.70 is adopted. Furthermore, a  $\Phi$  factor of 0.50 is recommended for FRP rupture-controlled failure. While a concrete crushing failure mode can be predicted based on calculations, the member as constructed may not fail accordingly. For example, if the concrete strength is higher than specified, the member can fail due to FRP rupture. For this reason and in order to establish a transition between the two values of  $\Phi$ , a section controlled by concrete crushing is defined as a section in which the reinforcement ratio is greater than or equal to 1.4 times the balanced reinforcement ratio ( $\rho_f \geq 1.4 \rho_{fb}$ ) and a section controlled by FRP rupture is defined as one in which  $\rho_f < \rho_{fb}$ .

Minimum reinforcement for flexure. If a member is designed to fail by FRP rupture,  $\rho_f < \rho_{fb}$ , a minimum amount of reinforcement,  $A_{f,min}$ , should be provided to prevent failure upon concrete cracking (that is,  $\Phi M_n \geq M_{cr}$  where  $M_{cr}$  is the cracking moment). The minimum reinforcement area is obtained by multiplying the existing ACI 318 limiting equation for steel by 1.8 (i.e.,  $1.8 = 0.90/0.50$  which is the  $\Phi$  ratio).

Crack width. For FRP-reinforced members, the crack width,  $w$ , can be calculated from the expression shown in ACI 318 with the addition of a corrective coefficient,  $k_b$ , for the bond quality. The  $k_b$  term is a coefficient that accounts for the degree of bond between the FRP bar and the surrounding concrete. For FRP bars having bond behavior similar to steel bars,  $k_b$  is assumed equal to one. Using the test results from Gao et al. (1998), the calculated values of  $k_b$  for three types of GFRP bars were found to be 0.71, 1.00, and 1.83. When  $k_b$  is not known, a value of 1.2 is suggested for deformed FRP bars.

Creep rupture and fatigue. Values for safe sustained and fatigue stress levels are 0.20, 0.30, and  $0.55 f_{fu}$  for glass, aramid and carbon fibers, respectively.

Shear. Several issues need to be addressed when using FRP as shear reinforcement, namely: FRP has a relatively low modulus of elasticity; FRP has a high tensile strength



and no yield point; tensile strength of the bent portion of an FRP bar is significantly lower than the straight portion; and FRP has low dowel resistance.

According to ACI 318, the nominal shear strength of a steel-RC cross section,  $V_n$ , is the sum of the shear resistance provided by concrete,  $V_c$ , and the steel shear reinforcement,  $V_s$ . Similarly, the concrete shear capacity  $V_{c,f}$  of flexural members using FRP as the main reinforcement can be derived from  $V_c$  multiplied by the ratio between the axial stiffness of the FRP reinforcement ( $\rho_f E_f$ ) and that of steel reinforcement ( $\rho_s E_s$ ). For practical design purposes, the value of  $\rho_s$  can be taken as  $0.5\rho_{s,max}$  or  $0.375\rho_b$ . Considering a typical steel yield strength of 420 MPa (60 ksi) for flexural reinforcement, the equation for  $V_{c,f}$  is that shown below (noting  $V_{c,f}$  cannot be larger than  $V_c$ ).

$$V_{c,f} = \frac{\rho_f E_f}{90 \beta_1 f'_c} V_c$$

The ACI 318 method used to calculate the shear contribution of steel stirrups,  $V_s$ , is applicable when using FRP as shear reinforcement with the provision that the stress level in the FRP shear reinforcement,  $f_{fv}$ , should be limited to control shear crack widths, maintain shear integrity of the concrete, and avoid failure at the bent portion of the FRP stirrup,  $f_{fb}$ . The stress level in the FRP shear reinforcement at ultimate for use in design is given by  $f_{fv} = 0.002 E_f \leq f_{fb}$ . An expression for  $f_{fb}$  is given in ACI 440.1R-01.

Development Length. The development length of FRP reinforcement can be expressed as shown below. This should be a conservative estimate of the development length of FRP bars controlled by pullout failure rather than concrete splitting.

$$\lambda_{bf} = \frac{d_b f_{fu}}{2700}$$

Manufacturers can furnish alternative values of the required development length based on substantiated tests conducted in accordance with available testing procedures. Reinforcement should be deformed or surface-treated to enhance bond characteristics with concrete.

It should be noted that the ACI 440 design guidelines specify different reduction factors for flexure and shear. For flexure, the proposed strength reduction factor proposed by the committee depends on the failure mode of the FRP reinforced section.

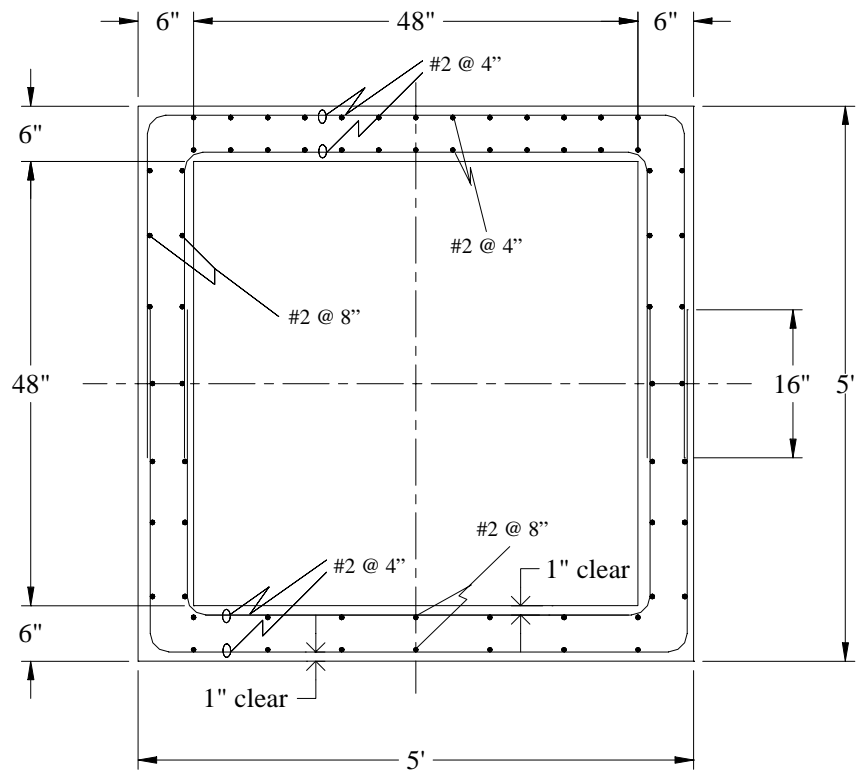


**Figure 2.1:** Details and GFRP reinforcement for box culvert.

### 3. FABRICATION AND INSTALLATION OF THE BOX CULVERT UNITS

A concrete pipe precaster fabricated the box culvert units. The bar manufacturer pre-bent and cut the reinforcing GFRP bars to the required shapes. The bars were tied together using plastic ties, as shown in Figure 3.1. Figure 3.2 shows a completed cage prior to casting. Two box units were instrumented with strain gages for laboratory testing purposes (see Figure 3.3). The specified concrete strength was 5,000 psi. Conventional concrete made of portland cement, fly ash, water, and Missouri River aggregate with a maximum aggregate size of 3/8 in was used to cast the box units. These materials were combined in a systematic manner, using predetermined quantities and proportions to ensure the desired concrete strength. The box units were cast using steel forms consisting of an exterior shell and an interior core, as shown in Figure 3.4. Plastic wheel spacers were used to maintain a cover thickness of 1 in, as shown in Figure 3.5. The concrete boxes were cast using a dry cast process with low frequency-high amplitude vibration to densely compact the mix in the form. The vibrators were directly attached to the central core of the form. The form was removed immediately as the newly formed box could support itself. The boxes were manufactured with tongue and groove joints. A typical box unit of this type is shown in Figure 3.6.



**Figure 3.1:** Rig of wood for GFRP cage assembly.



**Figure 3.2:** Finished GFRP cage.

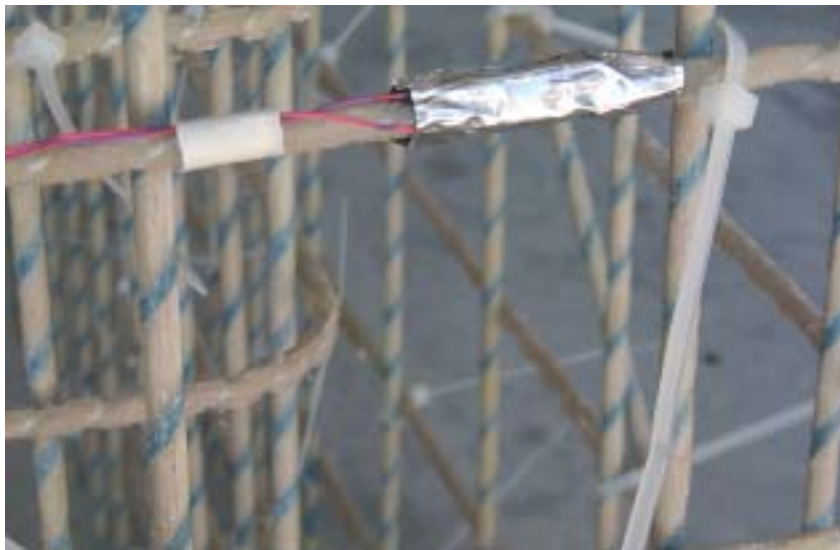


**Figure 3.3:** Strain gage on a GFRP bar.



(a) Interior core



(b) Exterior shell

**Figure 3.4.** Casting form.



**Figure 3.5:** Plastic wheel spacers.



**Figure 3.6:** A typical tongue and groove rectangular box section.



## 4. LABORATORY VERIFICATION

### 4.1. General

In addition to quality control tests conducted by the precaster, eight standard cylinders were acquired from different concrete batches used for the construction of the boxes and tested in the laboratory to determine the compressive strength of the concrete. The average strength of concrete cylinders at 28 days was 6,190 psi.

### 4.2. Test Set-up and Instrumentation

Two box culvert units (Box 1 and Box 2) were instrumented and tested in the laboratory. The test setup and instrumentation are shown in Figure 4.1. The two specimens were identical to the units installed in the field. Each specimen was instrumented with five Linear Variable Differential Transformers (LVDT's) to measure deformations. Load was applied using a hydraulic jack that reacted against a steel beam anchored to the strong floor using two high-strength threaded steel rods. The load was distributed across the top slab at mid-span using a steel beam. Load measurement was obtained using a load cell. Specimens were tested to failure by applying quasi-static load cycles in which the magnitude of the maximum load used in each successive load cycle was incremented until mid-span deflection of the top slab became excessive and failure signs were observed.

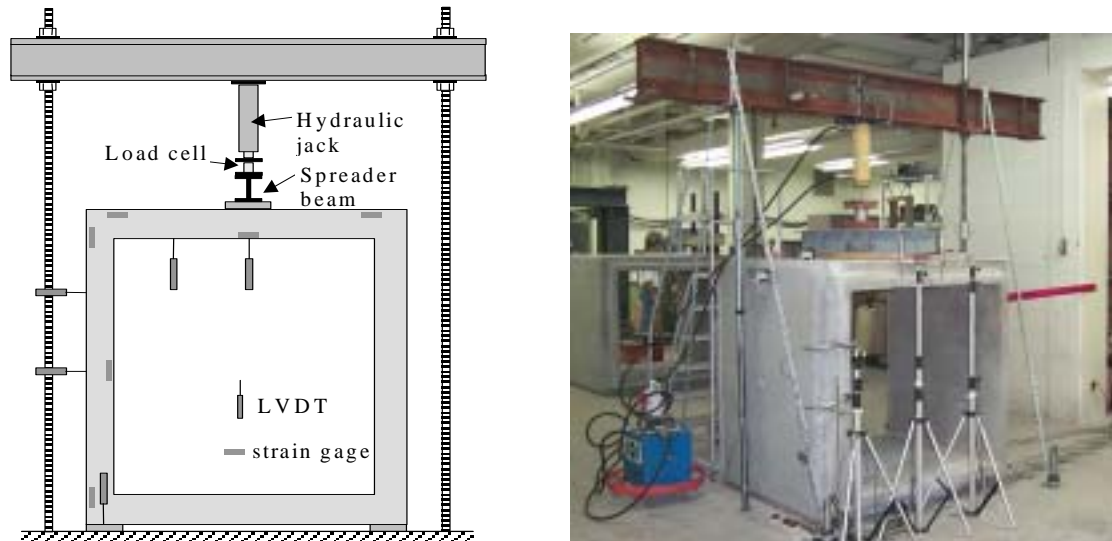


**Figure 4.1:** Test setup and instrumentation.

### 4.3. Test Results and Discussion

For Box 1, the first crack occurred at mid-span of the top panel at approximately 28 kips. This cracking load was comparable with the theoretical cracking load of 25 kips, computed based on elastic behavior. The next cracks occurred in the negative moment region at the top of the wall panels. Two cracks occurred simultaneously on both walls at approximately 32 kips. Final cracks occurred at the negative moment region of the top slab panel at approximately 35 kips, the maximum load attained during the test. Figure 4.2 shows the location and sequence of the cracks. Box 2 exhibited similar behavior with cracks occurring at approximately 24, 31, and 34 kips, respectively. Mid-span deflection envelopes for test boxes are shown in Figures 4.3 and 4.4. Typical strains measured on the GFRP reinforcement are shown in Figures 4.5 and 4.6, including the loading/unloading cycles.

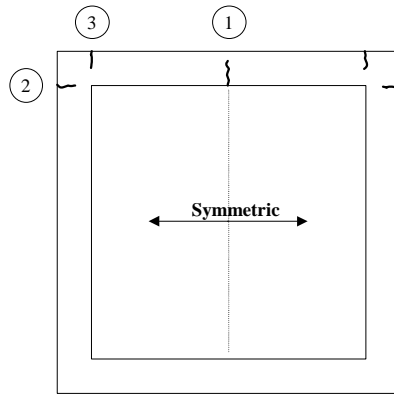


**Figure 4.2:** Cracking locations.

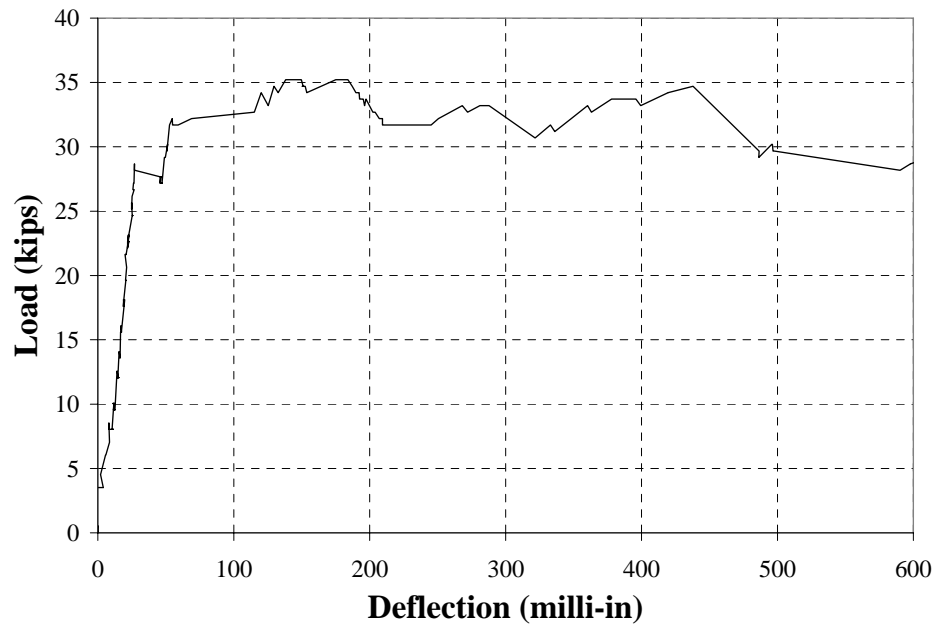


**Figure 4.3:** Mid-span load deflection of Box 1.

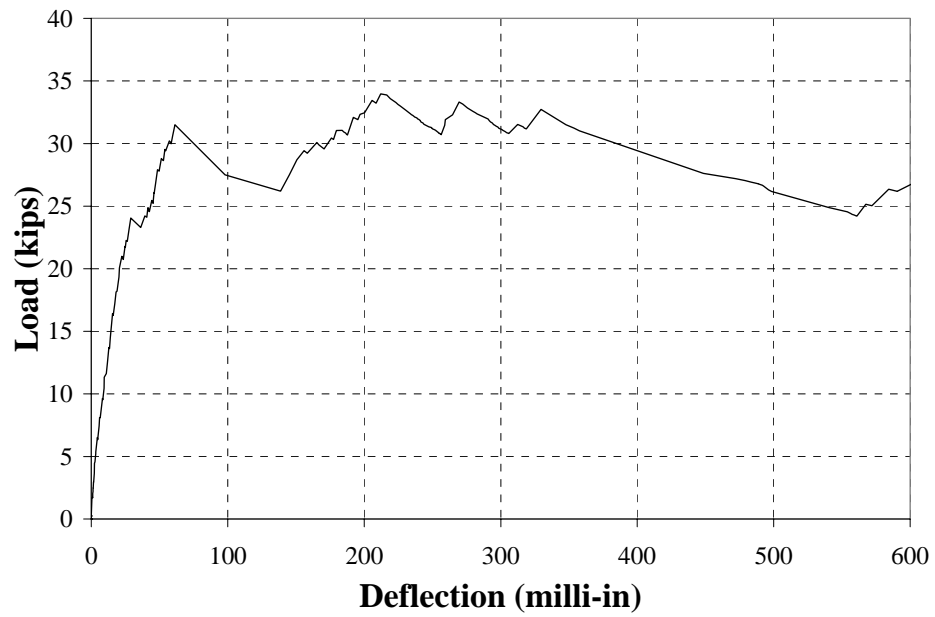


**Figure 4.4:** Mid-span load deflection of Box 2.

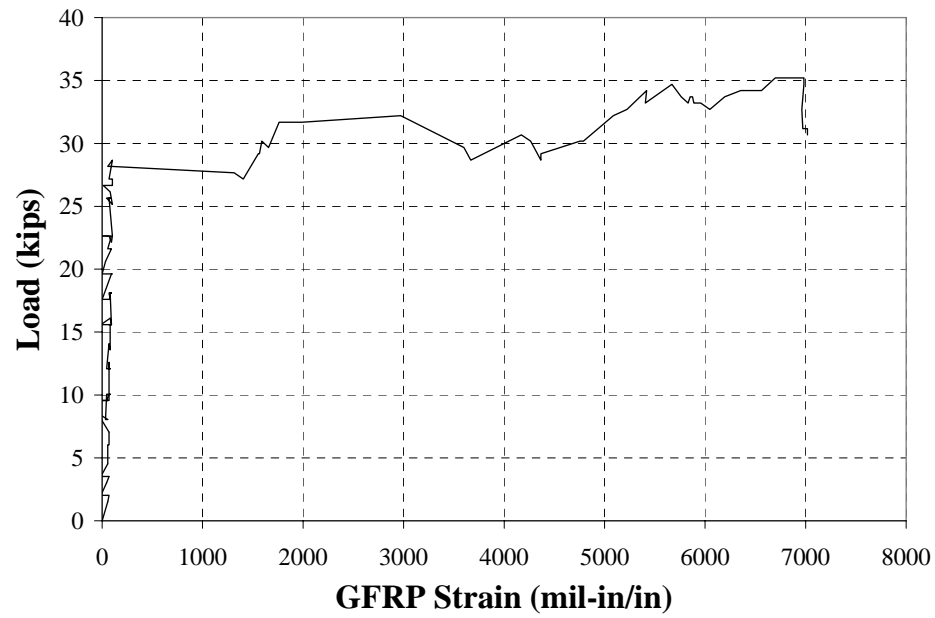


**Figure 4.5:** Strain measured at mid-span of Box 1.



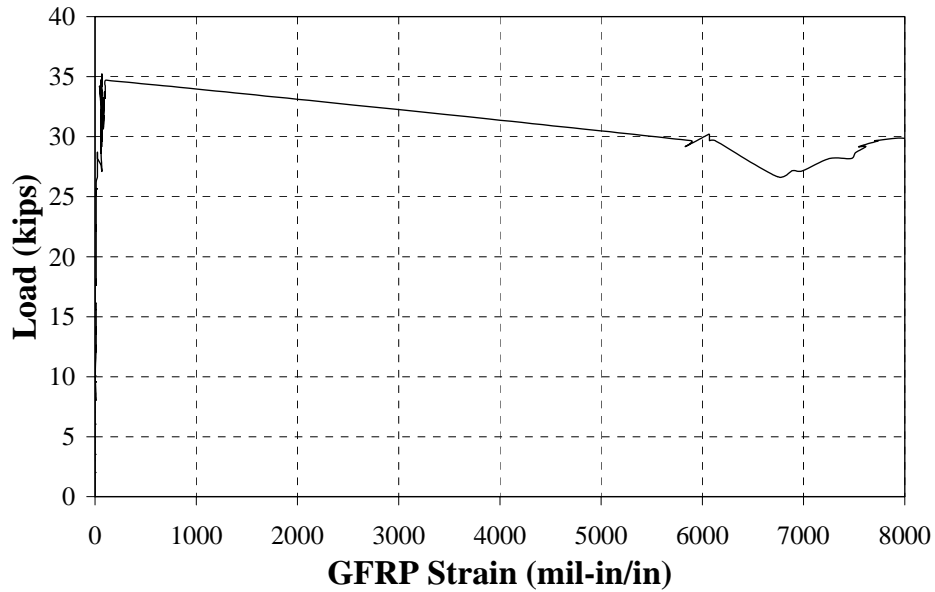


**Figure 4.6:** Strain measured at end of top panel for Box 1.

#### 4.4. Numerical Model

The box was modeled using Visual Analysis, a commercially available structural analysis software package. The model consists of a three-dimensional mesh of horizontal and vertical shell elements with thickness equal to the thickness of the box walls. Pin supports were assumed for the nodes at the bottom end of the wall panel on one side, and roller supports on the wall on the other side. The load applied to the model consisted of a uniform strip load distributed at mid-span of the top panel over a width of 6 in (simulating the load configuration adopted for the laboratory tests). Since the software is limited to linear elastic analysis, the behavior of the box unit after cracking was investigated by using elements with reduced stiffness at crack locations. The width of these elements was arbitrarily taken as 3 in, while their new thickness was calculated such that their moment of inertia was equal to that of a cracked section.

The load was applied to the model and mid-span deflection of the top slab was recorded for every load increment. When the applied load was equal to a cracking load, elements at crack locations were modified as indicated above. This procedure was continued until the full load–deflection diagram was obtained. Numerical results indicated that the maximum moment at top panel mid-span due to a total applied load of 35 kips was approximately 84.4 in-k/ft. This value was comparable to the nominal strength of the section computed analytically without reduction factors, which was 79.6 in-k/ft. The moment distribution in the model at maximum load is shown in Figure 4.7. Figure 4.8 illustrates a comparison of theoretical and experimental results of the two boxes where a good correlation can be observed.

Shown in this Figure 4.8 is also the load that would correspond to the ultimate moment  $M_u$  (i.e., 35.44 in-k/ft) as determined by BOXCAR.

#### 4.5. Comparison with Proposed Design Approach by ACI Committee 440H

According to the ACI Committee 440 guide (2001), the design tensile strength of GFRP bars  $f_{fu}$  for reinforcement of concrete exposed to earth and weather should be taken as  $0.7f_{fu}^*$ . The nominal capacity of an FRP reinforced flexural member  $M_n$  in which failure is governed by FRP rupture can be conservatively calculated using the following expressions:

$$M_n = 0.8A_f f_{fu} \left( d - \frac{\beta_1 c_b}{2} \right) \quad (3)$$

$$c_b = \left( \frac{\varepsilon_{cu}}{\varepsilon_{cu} + \varepsilon_{fu}} \right) d \quad (4)$$

in which,  $A_f$  is the area of FRP reinforcement,  $c_b$  is the depth of neutral axis at balanced strain condition,  $d$  is the depth of tensile reinforcement,  $f_{fu}$  is the design, and  $\varepsilon_{cu}$  is the ultimate strain of concrete for design taken as 0.003. For strength controlled by FRP rupture, the committee has proposed a strength reduction factor  $\phi$  of 0.5 to ensure adequate margin of safety against brittle-type failure. Using this approach, the design strength,  $\phi M_n$ , of the box panel is only 21.8 in-k/ft and 10.9 in-k/ft at mid-span and supports, respectively. In the latter case, the value of  $f_{fu}$  should be in fact replaced by  $0.5 f_{fu}$ , which corresponds to the tensile strength of the bar at the bent. Compared with the observed behavior of tested box units, these results are very conservative. Design based on the approach proposed by ACI Committee 440 would yield a stiffer member with a relatively high margin of safety against failure.

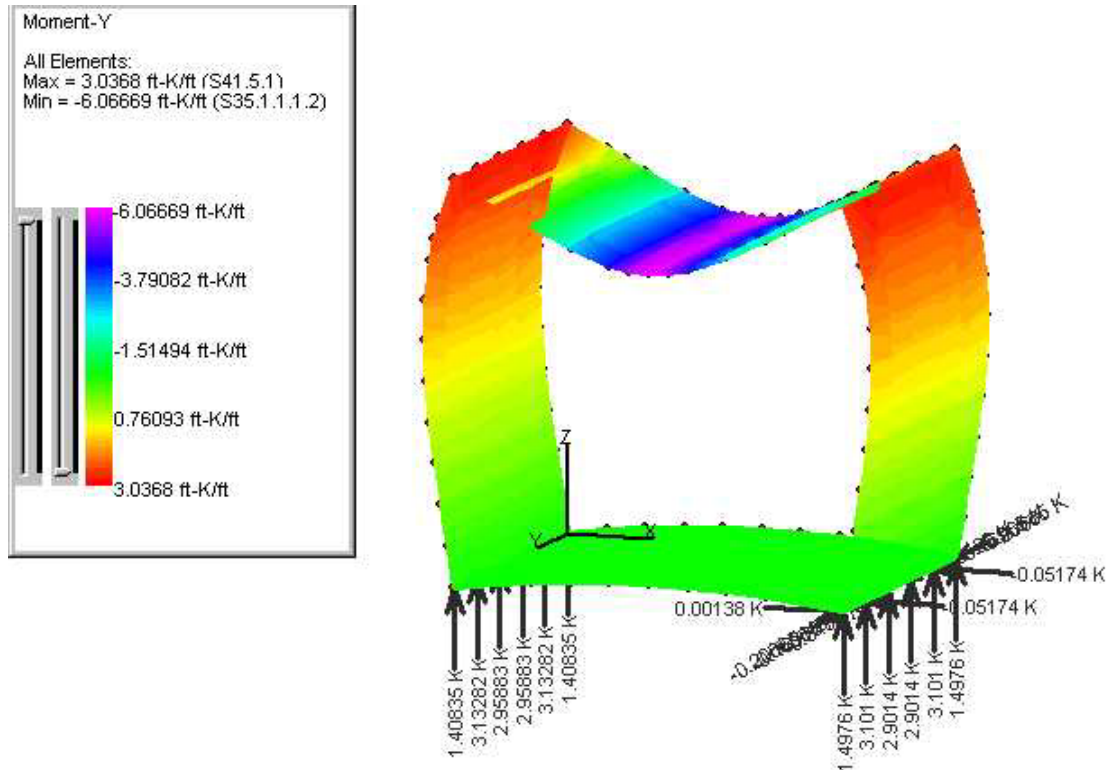


**Figure 4.7:** Theoretical moment distribution at maximum load.

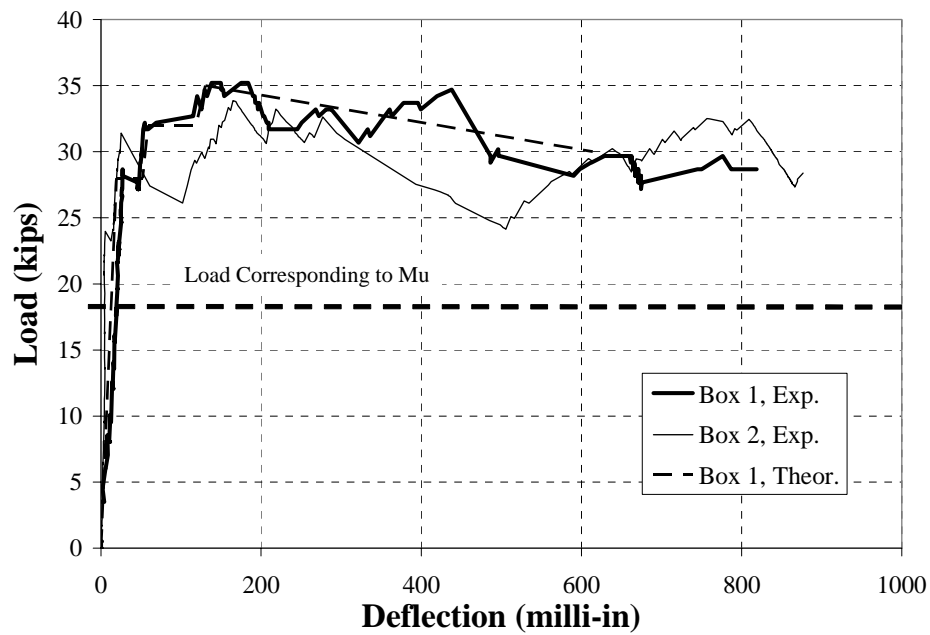


**Figure 4.8.** Comparison of experimental and theoretical load-deflection behavior.

## 5. BRIDGE CONSTRUCTION

The bridge was 36 ft wide and consisted of 18 precast concrete boxes arranged in two rows, nine boxes per row. A crew from Rolla City Public Work Department constructed the bridge, as shown in Figure 5.1. The new Walker Avenue Bridge was opened to traffic on October 13, 1999.

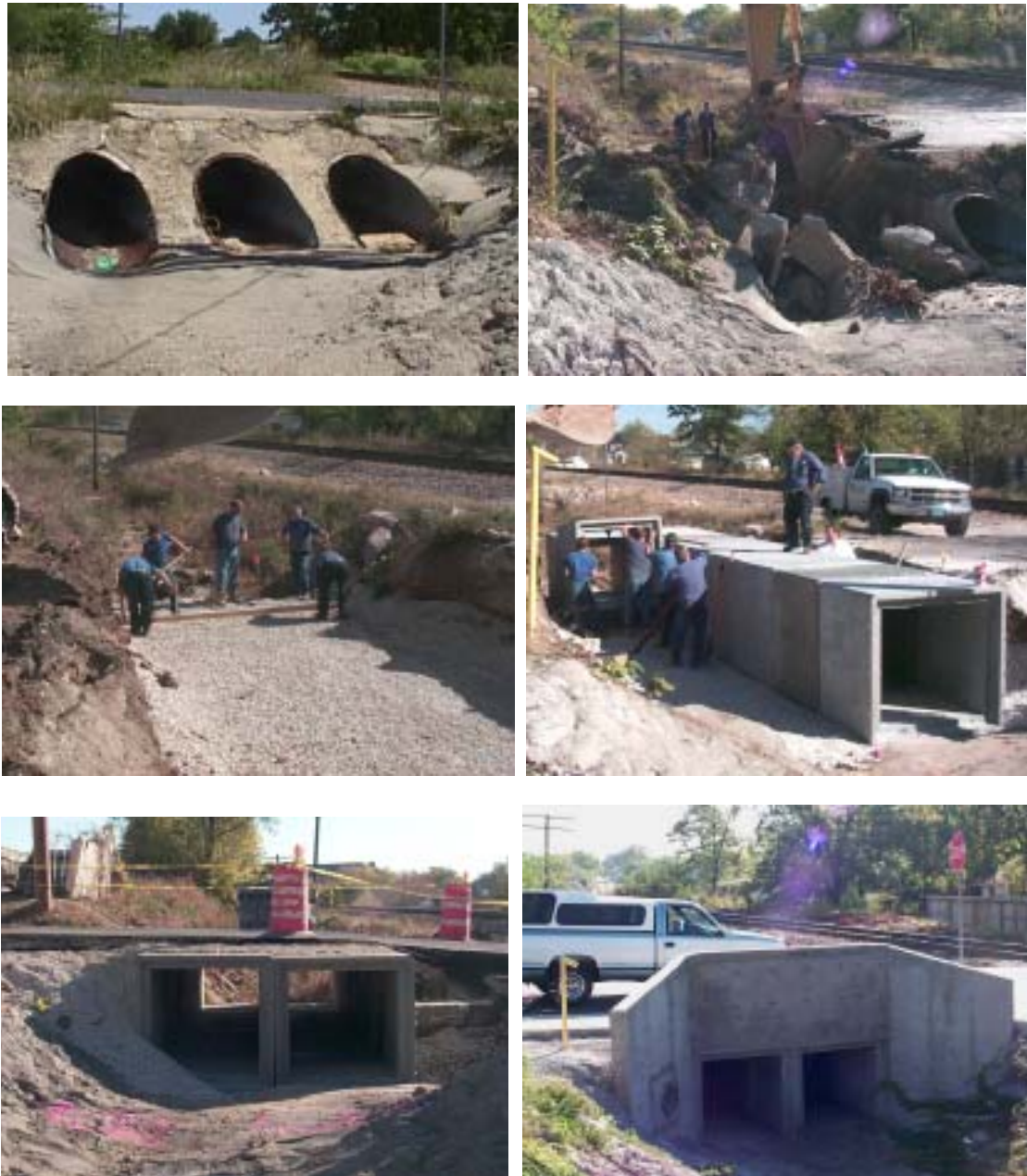


**Figure 5.1.** Bridge construction.

## 6. FIELD LOAD TESTING

### 6.1. General

The objective of the field load testing program was to evaluate the long-term performance of the concrete box culvert and add to current knowledge regarding the in-situ durability performance of GFRP concrete structures. Two load tests were performed by the UMR University Transportation Center to determine the bridge elastic deflection response. The first in-situ load test was performed on June 8, 2000 and the second load test on May 23, 2001.

### 6.2. Instrumentation

The load testing equipment consisted of a test vehicle, three LVDTs and their stands, three conditioner boxes to read LVDT's measurement, and a power generator. The vehicle used to load the bridge was a jet vacuum vehicle of 1000-gallon capacity. The vehicle was provided and weight-verified by the City of Rolla. For the first test, the test vehicle totaled 22.97 tons with a front axle load of 14,700 lbs. and a rear axle load of 30,250 lbs. For the second test, the test vehicle totaled 24.10 tons with a front axle load of 14,600 lbs. and a rear axle load of 33,600 lbs. A schematic of the vehicle used in this load test is shown in Figure 6.1. Deflection measurements at the center of the top panel of three adjacent RC boxes were taken using the LVDTs, as shown in Figure 6.2. The data was collected for five axle locations corresponding to the ends, quarter points, and midspan of the clear wall-to-wall distance on the transverse axis for both the north and south boxes of the bridge. Axle locations are also shown in Figure 6.2.

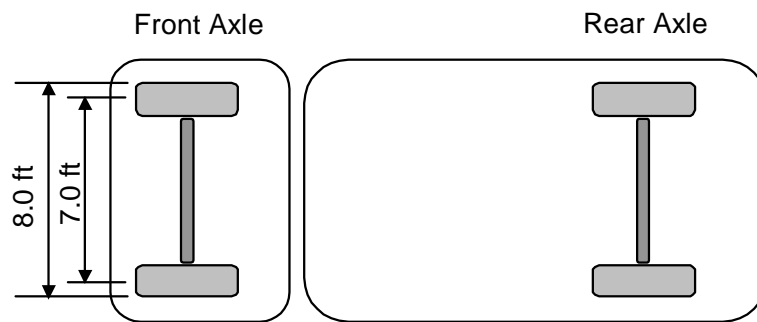


**Figure 6.1:** Test Truck Wheel Loads.

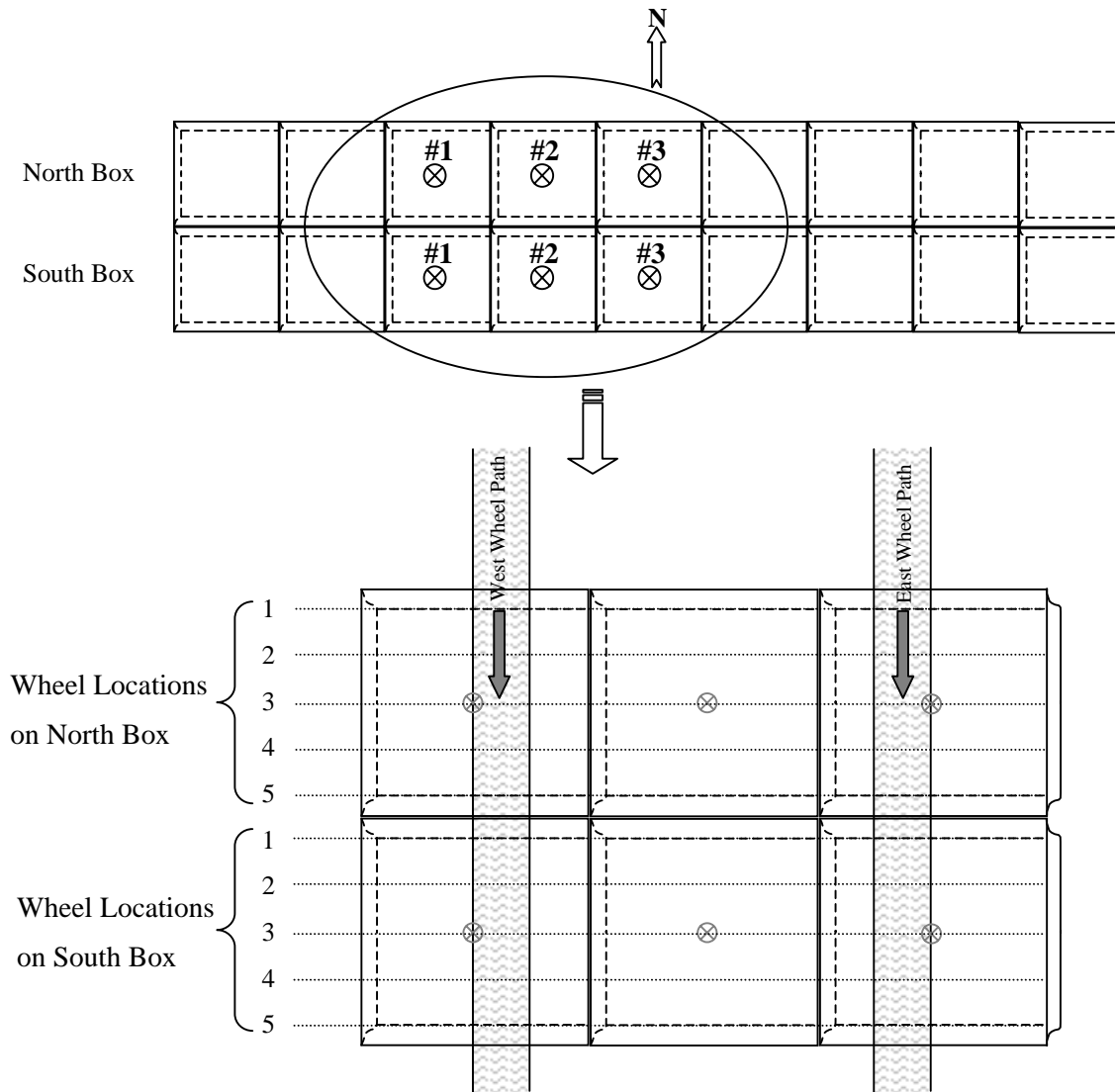


**Figure 6.2:** LVDT Layout and Axles Locations.

### 6.3. Load Testing

In each test, the truck made two passes over the bridge, one for each box. For each box (North and South), the test was performed by driving the truck at a crawl speed and stopping at each of the predetermined locations to measure the deflection of the box units (see Figure 6.3). The LVDTs were first set under the North Box. The truck was driven forward until the front wheel line coincided with the first mark (location 1). Deflection measurements were then taken at the three locations. The test vehicle was then moved to the following mark and deflection measurements were taken again. This process was continued until measurements were obtained for all the marks on the North box. The vehicle was then driven until the rear wheel line coincided with the first mark on the box. Deflection measurements were taken in a similar fashion to that of the front wheel. The test vehicle backed up for a few minutes until deflections measurements stabilized. The

LVDTs were then moved to the South box and the whole process was repeated to obtain deflections of the south box.



**Figure 6.3:** Field Load Testing.

#### 6.4. Test Results

Table 1 presents the results of the first load test for the North Box. Maximum deflection due to front axle loading was 0.0081 in measured on LVDT #1 when the wheel line was at location 3 (mid-span). Maximum deflection due to rear axle loading was also measured on LVDT #1 when the wheel line was at location 3. Maximum deflection due to rear axle loading was 0.0161 in.

Table 2 presents the results of the first load test for the South Box. Maximum deflection due to front axle loading was 0.015 in on LVDT #1 when the wheel line was at location 3 (mid-span). Maximum deflection due to rear axle loading was 0.0233 in measured at a similar load location.

**Table 6.1:** Deflections for the North Box –Test 1.

Loading	Axle Location	LVDT Deflections (in)		
		#1	#2	#3
Front Axle	1	0.0026	0.0002	0.0022
	2	0.0059	0.0003	0.0043
	3	0.0081	0.0005	0.0045
	4	0.0072	0.0004	0.0041
	5	0.0039	0.0003	0.0023
Rear Axle	1	0.0043	0.0007	0.0043
	2	0.0098	0.0010	0.0083
	3	0.0161	0.0012	0.0086
	4	0.0129	0.0007	0.0062
	5	0.0077	0.0003	0.0034

**Table 6.2:** Deflections for the South Box –Test 1.

Loading	Axle Location	LVDT Deflections (in)		
		#1	#2	#3
Front Axle	1	0.0066	0.0003	0.0023
	2	0.0120	0.0007	0.0044
	3	0.0150	0.0006	0.0043
	4	0.0079	0.0005	0.0026
	5	0.0062	0.0001	0.0018
Rear Axle	1	0.0079	0.0022	0.0032
	2	0.0213	0.0033	0.0051
	3	0.0233	0.0034	0.0063
	4	0.0147	0.0019	0.0041
	5	0.0073	0.0007	0.0024

Table 3 presents the results of the second load test for the North Box. Maximum deflection due to front axle loading was 0.0081 in measured on LVDT #1 when the wheel line was at location 3 (mid-span). Maximum deflection due to rear axle loading was also measured on LVDT #1 when the wheel line was at location 3. Maximum deflection due to rear axle loading was 0.016 in.

Table 4 presents the results of the second load test for the South Box. Maximum deflection due to front axle loading was 0.0145 in on LVDT #1 when the wheel line was at location 3 (mid-span). Maximum deflection due to rear axle loading was 0.022 in measured at similar load location.

Comparison of the maximum deflections for the two tests indicates that no significant change of stiffness occurred over a period of approximately one year using similar truck loads.

**Table 6.3:** Deflections for the North Box –Test 2.

Loading	Axle Location	LVDT Deflections (in)		
		#1	#2	#3
Front Axle	1	0.0027	0.0006	0.002
	2	0.0059	0.0009	0.0042
	3	0.0081	0.0012	0.0049
	4	0.0069	0.0009	0.0041
	5	0.0032	0.0005	0.0023
Rear Axle	1	0.0046	0.0019	0.0046
	2	0.0104	0.0044	0.008
	3	0.0160	0.0055	0.0082
	4	0.0123	0.0042	0.0062
	5	0.0070	0.0017	0.0038



**Table 6.4:** Deflections for the South Box –Test 2.

Loading	Axle Location	LVDT Deflections (in)		
		#1	#2	#3
Front Axle	1	0.0085	0.0004	0.0009
	2	0.0120	0.0005	0.0039
	3	0.0145	0.0006	0.0065
	4	0.0132	0.0004	0.0055
	5	0.0091	0.0003	0.0025
Rear Axle	1	0.0100	0.0012	0.0019
	2	0.0169	0.0026	0.0062
	3	0.0220	0.0037	0.0103
	4	0.0193	0.0031	0.0092
	5	0.0121	0.0011	0.0056

### 6.5. Load Deflection Characteristics

For both tests, eight months after construction and 20 months after construction, the measured deflections are very small indicating minimal cracking in the box units. As seen from the test data, the measured deflections on the three consecutive box units were not uniform. Box units subjected to similar loading configuration (e.g., at LVDT #1 and LVDT #3) measured larger deflections on LVDT #1 for both front and rear axle loading and on both North and South bridge boxes. A number of cracks were observed on these box units. Their larger deflections could therefore be related to a lower flexural stiffness due to cracking. Deflections measured on the middle box unit (LVDT #2) were always less than those measured on the other two units (LVDT #1 and LVDT #3). This behavior indicates that only a portion of the applied load is transferred from the loaded unit to an adjacent unit. Comparison of the measured load-deflection curves during load tests are shown in Figures 6.4 through 6.7. The LVDT numbers in these figures correspond to those shown in Figure 6.3. The notation 00 or 01 in the legend indicates the year of testing (e.g., 2000 or 2001).

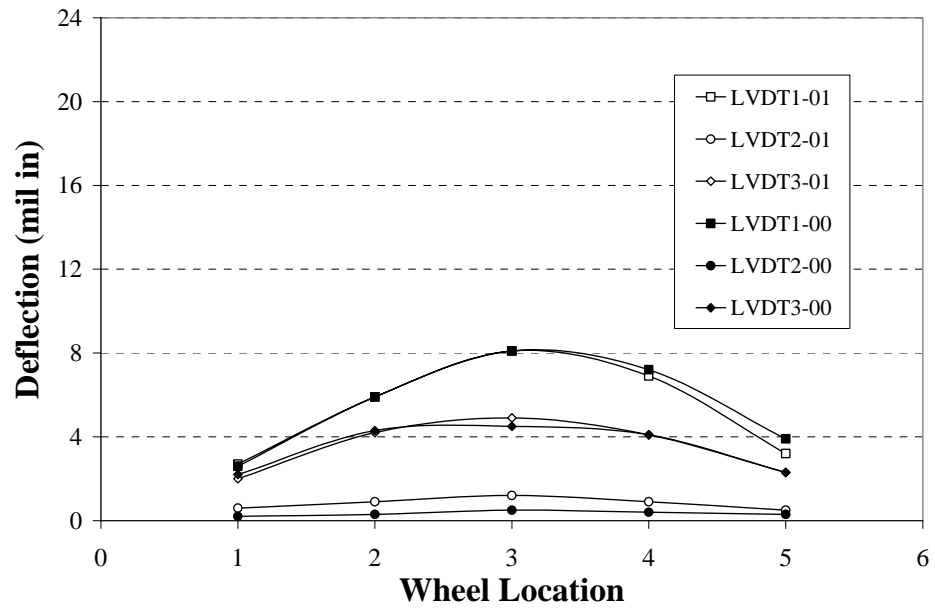


**Figure 6.4:** Deflections of the North Box Due to Front Axle Loading.

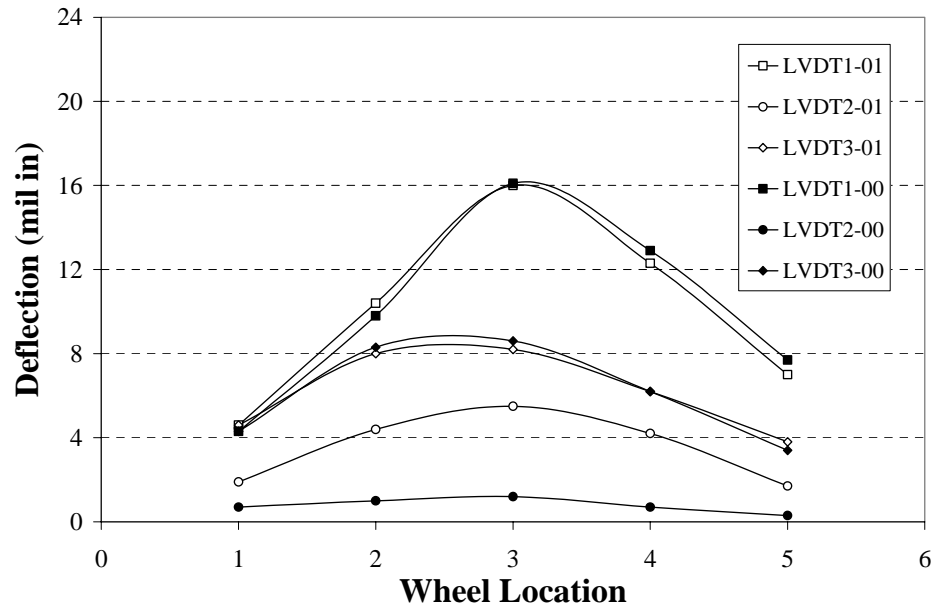


**Figure 6.5:** Deflections of the North Box Due to Rear Axle Loading.

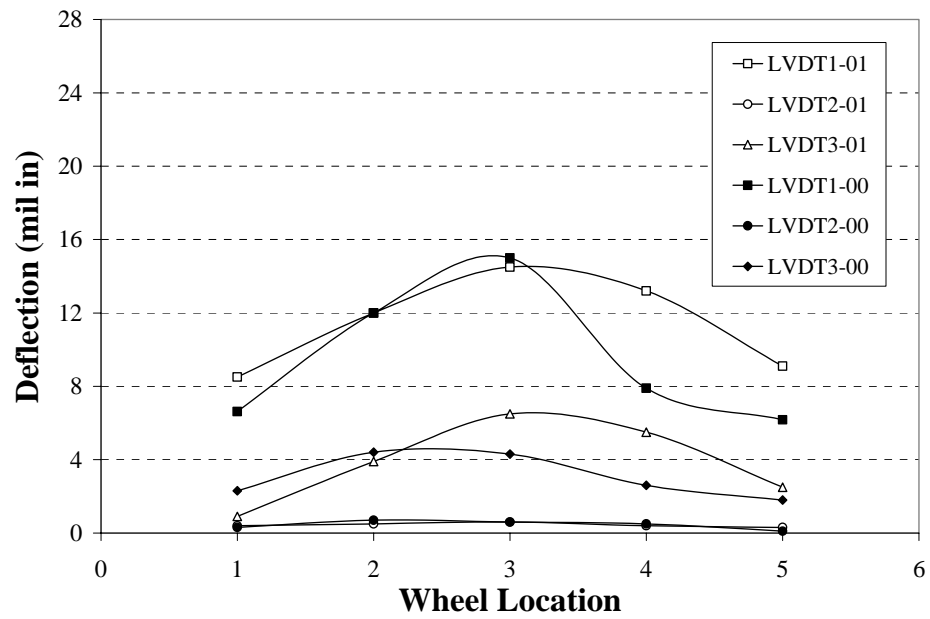


**Figure 6.6:** Deflections of the South Box Due to Front Axle Loading.

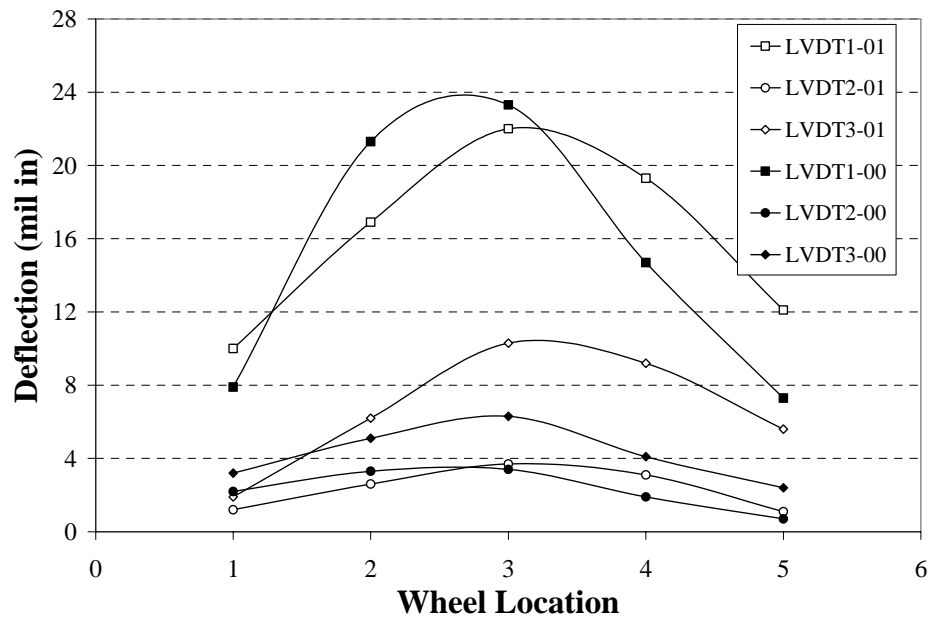


**Figure 6.7:** Deflections of the South Box Due to Rear Axle Loading.

Figures 6.8 and 6.9 show a comparison of the average reading of LVDT 1 and 3 for each box. Deflection readings of the test conducted in the year 2000 were adjusted by the ratio of the axle load for the two tests.

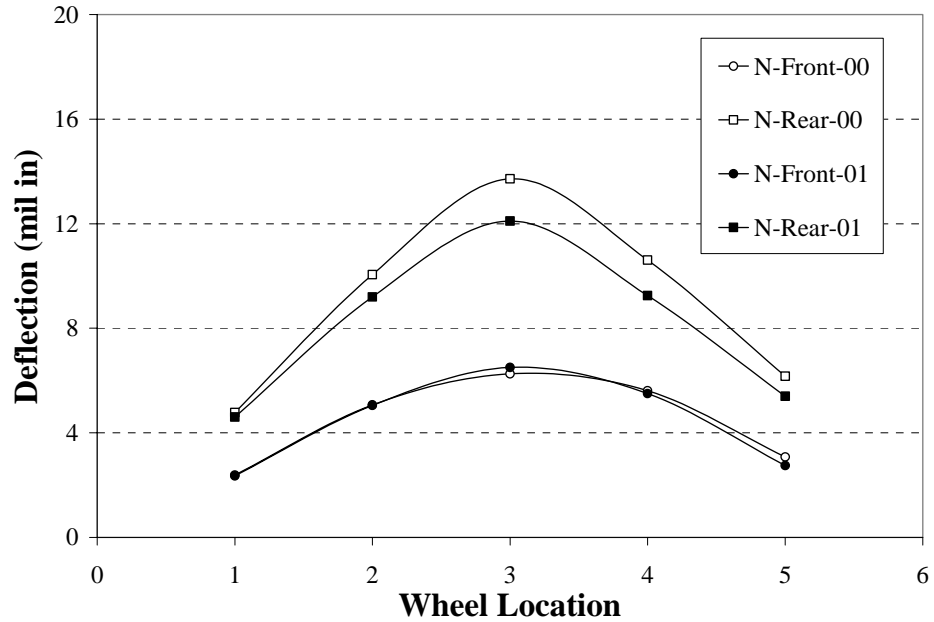


**Figure 6.8:** Adjusted Average for Measurements Taken on the North Box.

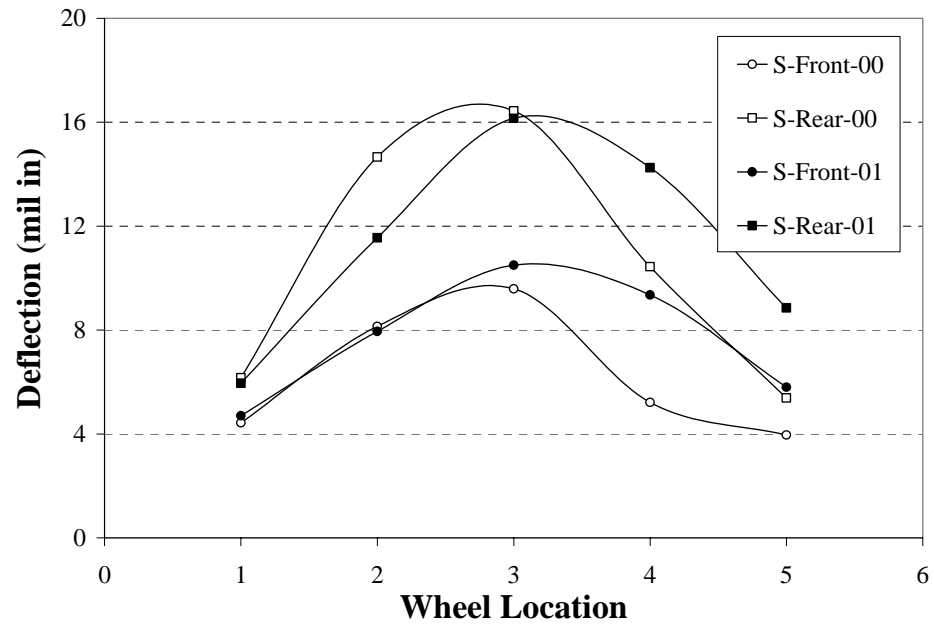


**Figure 6.9:** Adjusted Average for Measurements Taken on the South Box.

## **6.6. Summary**

Two elastic load tests were conducted for the newly constructed Walker Avenue Bridge. These tests are the first two of a series of field load tests aiming at monitoring the performance of the bridge over the course of three years. A measure of bridge performance is then determined by calculating the change in the elastic deflections. To ensure an accurate measure of performance, load tests should be conducted under similar loading and weather conditions.

The first load test was conducted 8 months after bridge construction while the second test was conducted 20 months after bridge construction. In each test, a jet vac truck was used to load the bridge. The performed load tests indicated that bridge deflections were small. For both tests, elastic deflection of the box units located under the west wheel path were higher than those obtained under the east wheel path under similar conditions. Variation in the elastic response of box units under similar loading condition was related to minor cracks that were observed on these boxes. After the load was removed, the original measurements were obtained again indicating elastic bridge behavior. Comparison of the results of the two tests indicates that no significant degradation of stiffness occurred during the past 12 months. Results obtained from these two tests will be used as a benchmark.

## **7. CONCLUSIONS**

This report presents the design, construction, and laboratory/field testing of a concrete box culvert bridge reinforced with internal glass FRP bars. Box units were designed for ultimate failure controlled by GFRP rupture using equilibrium and compatibility equations.

Laboratory testing indicated that the design approach is accurate and conservative and the experimental displacement behavior compared well with theoretical values obtained by numerical modeling. The design approach proposed by ACI Committee 440H is very conservative and, when implemented, would yield a stiffer member.

The in-situ load test of the bridge indicated that bridge deflections were small. Elastic deflection of the box units located under the west wheel path were higher than those obtained under the east wheel path. Variation in the elastic response of box units under similar loading conditions was related to the presence of minor cracks. After the load was removed there were no residual deflections. Results obtained from these field tests will be used as a benchmark. Comparison of the maximum deflections for the two tests indicates that no significant change of stiffness occurred over a period of approximately one year. It is envisioned that in-situ load tests will continue for at least three more years.

It is recommended that similar projects be undertaken in order to determine the cost benefits of this technology. This project only addressed the technical feasibility.

## 8. REFERENCES

- AASHTO (1996), "Standard Specifications for Highway Bridges," Sixteenth Edition, American Association of State Highway and Transportation Officials, Washington, D.C.
- ACI Committee 440, (1996), "State-of-the-Art Report on FRP for Concrete Structures," ACI440R-96, Manual of Concrete Practice, ACI, Farmington Hills, MI, 68 pp.
- ACI Committee 440 (2001), "Guide for Design and Construction of Concrete Reinforced with FRP bars," ACI440.1R-01, American Concrete Institute, Farmington Hills, Michigan, 41 pp.
- ASTM C 789-98, (1998) "Precast Reinforced Concrete Box Sections for Culverts, Storm Drains, and Sewers," American Society of Testing and Materials, ASTM, West Conshohocken, Pennsylvania.
- ASTM C 850-95a, (1995), "Precast Reinforced Concrete Box Sections for Culverts, Storm Drains, and Sewers with Less Than 2 ft of Cover Subjected to Highway Loading," American Society of Testing and Materials, ASTM, West Conshohocken, Pennsylvania.
- ASTM C 1433-00, (2000), "Standard Specification for Precast Reinforced Concrete Box Sections for Culverts, Storm Drains, and Sewers," American Society of Testing and Materials, ASTM, West Conshohocken, Pennsylvania.
- Benmokrane, B., Chaallal, O., and Masmoudi, R., (1996), "Flexural Response of Concrete Beams Reinforced with FRP Reinforcing Bars," *Structural Journal*, V. 93, No. 1, pp. 46-55.
- Benmokrane, B., (1997), "Bond Strength of FRP Rebar Splices," Proceedings of the Third International Symposium on Non-Metallic (FRP) Reinforcement for Concrete Structures (FRPRCS-3), Japan Concrete Institute, Sapporo, Japan, V. 2, pp. 405-412.
- Benmokrane, B., and Rahman, H., Eds., (1998), "Durability of Fiber Reinforced Polymer (FRP) Composites for Construction," *Proceedings of the First International Conference (CDCC '98)*, Quebec, Canada, 692 pp.
- Dolan, C.W., Rizkalla, S., and Nanni, A., Eds., (1999), "Fiber-Reinforced-Polymer Reinforcement for Reinforced Concrete Structures, SP-188," American Concrete Institute, Farmington Hills, MI, 1182 pp.
- Ehsani, M.R.; Saadatmanesh, H.; and Tao, S., (1996), "Design Recommendation for Bond of GFRP Rebars to Concrete," *Journal of Structural Engineering*, V. 122, No. 3, pp. 247-257.
- El-Badry, M., Ed., (1996), "Advanced Composite Materials in Bridges and Structures," Proceedings ACMBBS-II, Montreal, Canada, pp. 1027.
- Federal Highway Administration, (1989), "BOXCAR User and Programmer Manual," Version 1.0, Publication No. FHWA-IP-89-018, Turner-Fairbanks Highway Research Center, McLean, Virginia, 231 pp.

- Gao, D.; Benmokrane, B.; and Tighiouart, B., (1998), "Bond Properties of FRP Rebars to Concrete," *Technical Report*, Department of Civil Engineering, University of Sherbrooke, Sherbrooke (Quebec), Canada, pp. 27.
- Heger, F.J. and Long, K.N., (1976), "Structural Design of Precast Concrete Box Sections to Support Surface Highway Wheel Loads with Zero to Deep Earth Cover," presented at ASTM Committee C-12 Symposium on Concrete Pipe, Chicago, IL.
- Iyer, S.L. and R. Sen, Editors (1991), "Advanced Composite Materials in Civil Engineering Structures," Proc., American Society of Civil Engineers, New York, NY, 443 pp.
- Japan Society of Civil Engineers (JSCE), (1997), *Proceeding of the Third International Symposium on Non-Metallic (FRP) Reinforcement for Concrete Structures (FRPRCS-3)*, Japan Concrete Institute, Sapporo, Japan, Vol. 2, pp. 511-518.
- Japan Society of Civil Engineers (JSCE), (1997), "Recommendation for Design and Construction of Concrete Structures Using Continuous Fiber Reinforcing Materials," Concrete Engineering Series, No. 23, 325 pp.
- Nanni, A., Ed. (1993), Fiber-Reinforced-Plastic (FRP) Reinforcement for Concrete Structures: Properties and Applications, Developments in Civil Engineering, Vol. 42, Elsevier, Amsterdam, The Netherlands, pp. 450.
- Nanni, A. (1993). "Flexural Behavior and Design of Reinforced Concrete Using FRP Rods," *Journal of Structural Engineering*, 119:11, 3344-3359.
- Nanni, A. and Dolan, C.W., Eds. (1993), "FRP Reinforcement for Concrete Structures," Proc., ACI SP-138, American Concrete Institute, Detroit, MI, pp. 977.
- Rizkalla, S.H., (1997), "A New Generation of Civil Engineering Structures and Bridges," *Proceedings of the Third International Symposium on Non-Metallic (FRP) Reinforcement for Concrete Structures (FRPRCS-3)*, Sapporo, Japan, Vol. 1, pp. 113-128.
- Saadatmanesh, H., and Ehsani, M. R., Eds., (1998), "Fiber Composites in Infrastructure," *Proceedings of the Second International Conference on Composites in Infrastructure (ICCI-98)*, Tucson, AZ.
- Tadros, G.; Tromposch, E.; and Mufti, A., (1998), "University Drive/Crowchild Trail Bridge Superstructure Replacement," *Second International Conference on Composites in Infrastructure (ICCI-98)*, Tucson, Arizona, Vol. 1, pp. 693-704.



## APPENDIX A: BRIDGE LOCATION

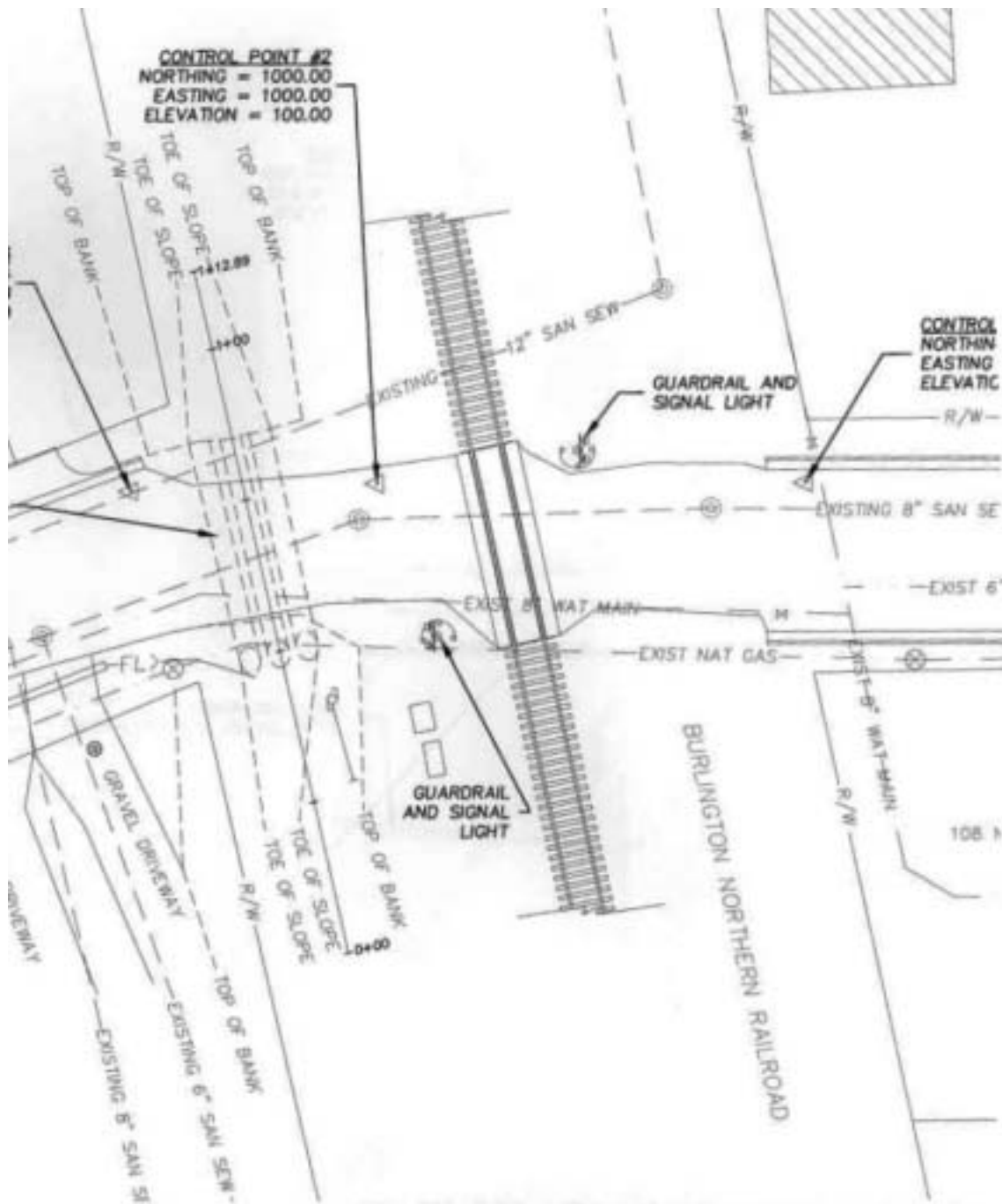


**Figure A1:** Current Walker Culvert plan

## APPENDIX B: SELECTED OUTPUT OF BOXCAR

AASHTO HS-15. 22.8 INCHES OF FILL  
TRAFFIC TRANSVERSE TO CULVERT FLOW

### ULTIMATE LOAD FORCES

SECTION (IN.-K/FT)	M+ (K/FT)	V+ (K/FT)	P+ (K/FT)	M- (K/FT)	V- (K/FT)	P- (K/FT)
1	33.11	0.61	-0.05	0	-0.61	-1.01
2	0	3.26	-0.59	-13.93	0	-0.48
3	0	3.26	-0.59	-13.93	0	-0.48
4	0	0	-1.02	-18.9	-1.44	-2.3
5	0	0	-1.02	-18.9	-1.44	-2.3
6	9.15	0.11	-1.02	-16.9	-0.07	-2.22
7	0	1.49	-1.02	-21.31	-0.01	-2.22
8	0	1.49	-1.02	-21.31	-0.01	-2.22
9	0	0	-0.45	-14.53	-3.61	-0.86
10	0	0	-0.45	-14.53	-3.61	-0.86
11	35.44	0.32	-0.11	0	-0.32	-1.19
12	6.88	2.73	-0.22	-5.75	0	-0.75
13	6.88	2.73	-0.22	-5.75	0	-0.75
14	0	0	-1.02	-16.15	-1.18	-2.36
15	0	0	-1.02	-16.15	-1.18	-2.36
16	0	1.25	-1.02	-18.11	0	-2.36
17	0	1.25	-1.02	-18.11	0	-2.36
18	7.13	0	-0.45	-5.37	-2.99	-0.45
19	7.13	0	-0.45	-5.37	-2.99	-0.45
20	0	3.66	-0.22	-23.46	0	-0.75
21	0	0	0	0	0	0
22	0	0	0	0	0	0
23	0	4.08	-0.44	-26.04	0	-0.45

CONCRETE SHEAR STRENGTH TAKEN AS 2.SQUARE ROOTS  $f_c$   
\*\*\*\*\* SHEAR DESIGN TABLE - METHOD 2 \*\*\*\*\*

DESIGN	SECTION	12	13	14	15
M/(V*PHI*D)		1.032	1.032	3.175	3.175
ULTIMATE (KIPS/FT)	SHEAR	2.728	2.728	1.18	1.18
ULTIMATE (KIPS/FT)	THRUST	0.476	0.476	2.297	2.297
STEEL RATIO		0.002462	0.002462	0.002462	0.002462
DEPTH TO (IN.)	STEEL	4.875	4.875	4.875	4.875

DISTANCE "A-END,"	FROM (IN.)	7.144	7.144	46.856	46.856
THRUST	FACTOR (FN)	0.976	0.976	0.8	0.8
DIAGONAL "STRENGTH,"	TENSION (KIPS/FT)	10.552	10.552	6.542	6.542
ULTIMATE ALLOWABLE	SHEAR/ SHEAR	0.259	0.259	0.18	0.18
NEW STEEL AREA TO DIAGONAL (SQ.IN./FT)	DUE TENSION	0	0	0	0
DESIGN	SECTION	16	17	18	19
M/(V*PHI*D)		3.444	3.444	0.971	0.971
ULTIMATE (KIPS/FT)	SHEAR	1.249	1.249	2.988	2.988
ULTIMATE (KIPS/FT)	THRUST	2.221	2.221	0.855	0.855
STEEL RATIO		0.002462	0.002462	0.002462	0.002462
DEPTH TO (IN.)	STEEL	4.875	4.875	4.875	4.875
DISTANCE "A-END,"	FROM (IN.)	7.144	7.144	46.856	46.856
THRUST	FACTOR (FN)	0.81	0.81	0.962	0.962
DIAGONAL "STRENGTH,"	TENSION (KIPS/FT)	6.461	6.461	11.04	11.04
ULTIMATE ALLOWABLE	SHEAR/0.193 SHEAR	0.193	0.271	0.271	
NEW STEEL AREA TO DIAGONAL NN(SQ.IN./FT)	DUE TENSION	0	0	0	0

BOX CULVERT DESIGN SUMMARY SHEET

\*\*\*\*\*

I N S T A L L A T I O  
N D A T A

HEIGHT OF FILL OVER "CULVERT, FT" 1.9

SOIL UNIT "WEIGHT," PCF 120

MINIMUM LATERAL SOIL PRESSURE COEFFICIENT 0.25

MAXIMUM LATERAL SOIL PRESSURE COEFFICIENT 0.5

SOIL - STRUCTURE INTERACTION COEFFICIENT 1.2

L O A D I N G D A T A

DEAD LOAD FACTOR - MOMENT AND SHEAR 1.3

DEAD LOAD FACTOR - THRUST 1

LIVE LOAD FACTOR - MOMENT AND SHEAR 2.17

LIVE LOAD FACTOR - THRUST 1

STRENGTH REDUCTION FACTOR-FLEXURE 0.7

STRENGTH REDUCTION FACTOR-DIAGONAL TENSION 0.85

LIVE LOAD TYPE AASHTO HS-15.  
DIRECTION OF VEHICLE TRAVEL RELATIVE

TO CULVERT FLOW TRANSVERSE

VERTICAL SURCHARGE "PRESSURE," PSF 0

HORIZ. SURCHARGE PRESSURE AT CULVERT "TOP," PSF 0

HORIZ. SURCHARGE PRESSURE AT CULVERT "BOTTOM," PSF 0

M A T E R I A L P R O  
P E R T I E S

CONCRETE - SPECIFIED COMPRESSIVE "STRENGTH," KSI 5

REINFORCING TYPE SMOOTH WELDED WIRE FABRIC

G E O M E T R Y					
TOP	SLAB	"THICKNESS,"	INCHES	6	
SIDE	WALL	"THICKNESS,"	INCHES	6	
BOTTOM	SLAB	"THICKNESS,"	INCHES	6	
HORIZONTAL	HAUNCH	"DIMENSION,"	INCHES	0	
VERTICAL	HAUNCH	"DIMENSION,"	INCHES	0	
CONCRETE	COVER OVER	"STEEL,"	INCHES		
TOP	SLAB	-	OUTSIDE	FACE	1
SIDE	WALL	-	OUTSIDE	FACE	1
BOTTOM	SLAB	-	OUTSIDE	FACE	1
TOP	SLAB	-	INSIDE	FACE	1
SIDE	WALL	-	INSIDE	FACE	1
BOTTOM	SLAB	-	INSIDE	FACE	1

#### BOXCAR Critical Sections for Flexure and Shear Design

